

Pursuit Tracking and Higher Levels of Skill Development in the Human Pilot

RONALD A. HESS

Abstract—A model of the human pilot is offered for pursuit tracking tasks; the model encompasses an existing model for compensatory tracking. The central hypothesis in the development of this model states that those primary structural elements in the compensatory model responsible for the pilot's equalization capabilities remain intact in the pursuit model. In this latter case, effective low-frequency inversion of the controlled-element dynamics occurs by feeding-forward derived input rate through the equalization dynamics, with low-frequency phase "droop" minimized. The sharp reduction in low-frequency phase lag beyond that associated with the disappearance of phase droop is seen to accompany relatively low-gain feedback of vehicle output. The results of some recent motion cue research are discussed and interpreted in terms of the compensatory-pursuit display dichotomy. Tracking with input preview is discussed in a qualitative way. In terms of the model, preview is shown to demand no fundamental changes in structure or equalization and to allow the pilot to eliminate the effective time delays that accrue in the inversion of the controlled-element dynamics. Precognitive behavior is discussed, and a model that encompasses all the levels of skill development outlined in the successive organizations of perception (SOP) theory is finally proposed.

I. INTRODUCTION

NEARLY ALL the manual control displays used in continuous tracking tasks can be classified as either "compensatory" or "pursuit" in nature, depending on the amount of information presented to the operator. Consider the functional block diagrams of Fig. 1, which represent a pair of single-axis tracking tasks (scalar system input and output). In Fig. 1(a), the operator is presented with a display of system error alone. This display, shown in Fig. 2(a), is referred to as compensatory. The visually displayed effects of the operator's responses are not distinguishable from the system input. In Fig. 1(b), the operator is presented with both system input and output. The corresponding display, shown in Fig. 2(b), is referred to as pursuit. Here the operator's corrective responses can be distinguished from his input. Note that system error can be easily inferred from the spatial separation of the "target" and "follower" symbols.

Examples of compensatory and pursuit displays abound in the manual-control literature [1]. However, the research to be described here is motivated by more than just the physical existence of compensatory and pursuit displays in manual control tasks. More subtle issues related to human skill development are also involved. In an elegant monograph published over 19 years ago, Krendel and McRuer

[2] postulated a successive organization of perception (SOP) theory for tracking skill development; the theory that the human's *internal* organizing functions occurring in skill development operate in a manner similar to the *external* changes in display characteristics one can effect in going from a compensatory to a pursuit display (Fig. 2(a) to (b)). Thus the comparative study of compensatory and pursuit tracking models of the human operator or pilot that follows may provide some insight into the mechanisms of skill development.

Despite the frequent occurrence of pursuit display formats and the implications of the SOP theory, most of the research in manual control, particularly pilot modeling, has concerned itself with the compensatory display situation (e.g., the study of [3]). This is primarily because the classical spectral measurement techniques, used in identifying pilot dynamics were not capable of uniquely identifying the more complex multistimulus models suggested by the pursuit display situation of Fig. 1(b). However, some very useful results were obtained by Elkind [4] and Wasicko *et al.* [5] in determining "equivalent" single-stimulus open-loop dynamics for the pursuit case. In addition, by adding a disturbance signal to the system, Allen and Jex [6] and Reid [7] were able to treat the multistimulus problem by measuring two distinct describing functions for pursuit tracking. Unlike the compensatory research of [3], however, this experimental pursuit work has not culminated in a definitive addition to manual control theory. Rather, it has served as more of an empirical addition to the general body of knowledge dealing with manual control.

It is the purpose of the research described herein to provide a structural model for pursuit tracking that is similar to the compensatory model introduced in [8] and refined in [9]. As in [9], it is hoped that such a model can provide 1) a theoretical framework within which a variety of empirical pilot-vehicle response phenomena can be interpreted, and 2) a control theoretic description of skill development. The next section will begin with a discussion of the describing-function data that have been obtained for tracking with pursuit displays and K/s^2 controlled-element dynamics. We will emphasize the differences between these describing functions and those obtained for tracking with compensatory displays. Following this, the compensatory model of [9] will be briefly reviewed, the aforementioned pursuit tracking model of the human pilot will be introduced, and a discussion of the results of some recent

Manuscript received May 16, 1980; revised January 6, 1981.

The author is with the Aircraft Guidance and Navigation Branch, Ames Research Center, NASA, Moffett Field, CA 94035.

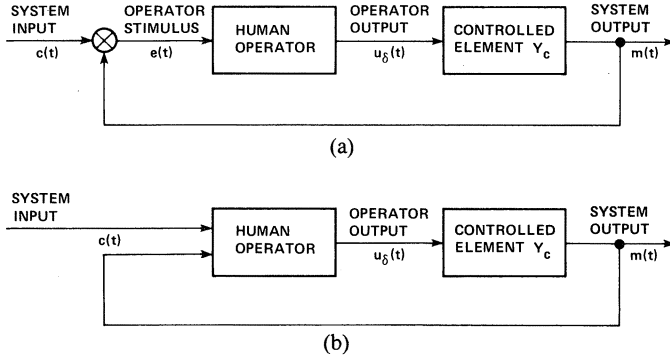


Fig. 1. Manual control systems. (a) Compensatory behavior. (b) Pursuit behavior.

motion-cue research will be undertaken in light of the pursuit model that has been developed. Finally, the implications of the model in tracking with preview and precognitive behavior will be discussed.

II. DATA SUMMARY, K/s^2 DYNAMICS

A very general block diagram, which summarizes the pilot's signal processing options in pursuit tracking, is shown in Fig. 3. The elements Y_c , Y_{p_e} , and Y_{p_m} are describing functions that indicate the operations on the three displayed variables, $c(t)$, $e(t)$, and $m(t)$, respectively. Solving for the pilot's output, system error, and system output yields

$$u_\delta = \left[\frac{Y_{p_e} + Y_{p_m}}{1 + Y_c(Y_{p_e} - Y_{p_m})} \right] c + \left[\frac{1}{1 + Y_c(Y_{p_e} - Y_{p_m})} \right] n_u, \quad (1)$$

$\Phi_{cu_\delta}/\Phi_{cc}$ $\Phi_{n_u u_\delta}/\Phi_{n_u n_u}$

$$e = \left[\frac{1 - Y_c(Y_{p_e} + Y_{p_m})}{1 + Y_c(Y_{p_e} - Y_{p_m})} \right] c - \left[\frac{Y_c}{1 + Y_c(Y_{p_e} - Y_{p_m})} \right] n_u, \quad (2)$$

Φ_{ce}/Φ_{cc} $\Phi_{n_u e}/\Phi_{n_u n_u}$

and

$$m = \left[\frac{Y_c(Y_{p_e} + Y_{p_m})}{1 + Y_c(Y_{p_e} - Y_{p_m})} \right] c + \left[\frac{Y_c}{1 + Y_c(Y_{p_e} - Y_{p_m})} \right] n_u, \quad (3)$$

Φ_{cm}/Φ_{cc} $\Phi_{n_u m}/\Phi_{n_u n_u}$

where Φ represents the power and cross power spectral densities of the variables appearing in the subscripts.

Now, as [5] points out, the ratio

$$Y_\beta = \frac{\Phi_{cm}}{\Phi_{ce}} = \frac{Y_c(Y_{p_e} + Y_{p_m})}{1 - Y_c(Y_{p_e} + Y_{p_m})} \quad (4)$$

has the property that the portions of m and e linearly correlated with the input are described by

$$\frac{m}{c} = \frac{Y_\beta}{1 + Y_\beta} \quad (5)$$

$$\frac{e}{c} = \frac{1.0}{1 + Y_\beta} \quad (6)$$

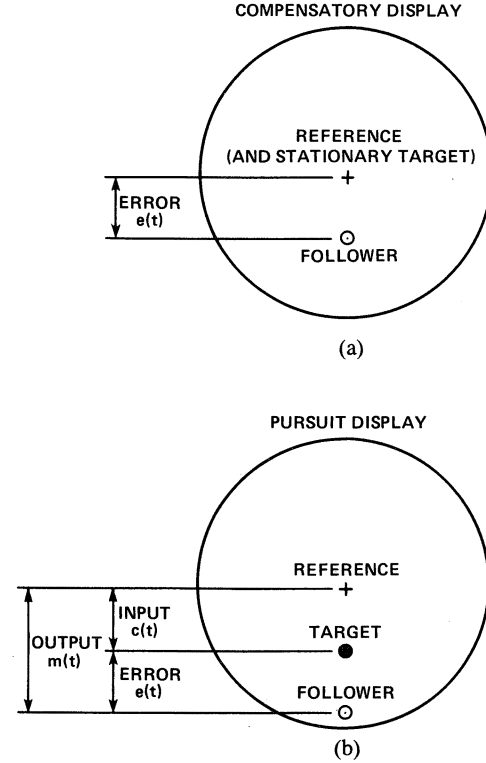


Fig. 2. Displays. (a) Compensatory. (b) Pursuit.

independent of the type of display or pilot utilization. Thus Y_β is the effective open-loop describing function; it has essentially the same interpretation in the pursuit as in the compensatory situation. That is, a single-loop closure about Y_β results in the closed-loop characteristics. Although unique measurement of the elements Y_{p_e} , Y_{p_m} , and Y_{p_m} is not possible with a single system input, Y_β is readily measurable and provides a function comparable to the measurements obtained for compensatory tracking [3].

As mentioned in the Introduction, the comparison of experimental compensatory and pursuit pilot describing functions will be restricted to those tracking tasks that utilize K/s^2 dynamics. This is done for two reasons. First, these higher order dynamics accentuate the differences in measured pilot describing functions between display conditions. Differences appear to exist for lower order controlled elements ($Y_c = K, K/s$); however, they are more subtle and less amenable to qualitative replication with a pilot model. Second, similar dynamics have been used in motion-cue research that will be discussed later.

Fig. 4 shows a comparison of pursuit and compensatory describing functions for $Y_c = K/s^2$ from [5]. The most immediate and striking difference in the data lies in the low-frequency phase results. For the compensatory case, the phase exhibits the well-known low-frequency phase "droop." For the pursuit case, however, the droop disappears, and phase lags are markedly decreased. Since only a single subject was used in [5], further corroboration of the qualitative difference in open-loop characteristics is desirable. This corroboration can be found in [6], a study in which four pilot subjects were used. Again, for K/s^2 dynamics, the open-loop Y_β measurements, shown in Fig.

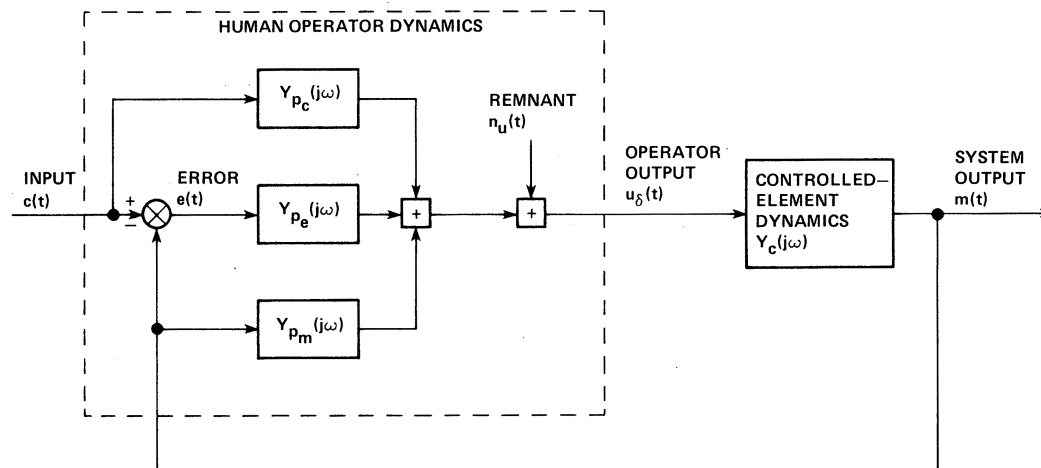


Fig. 3. General block diagram of human operator in pursuit display tracking task.

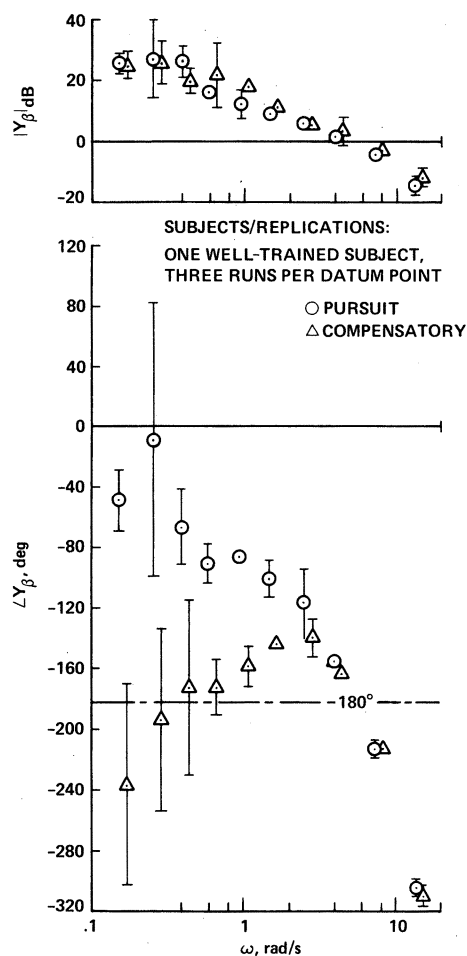


Fig. 4. Comparison of pursuit and compensatory display describing functions from [5].

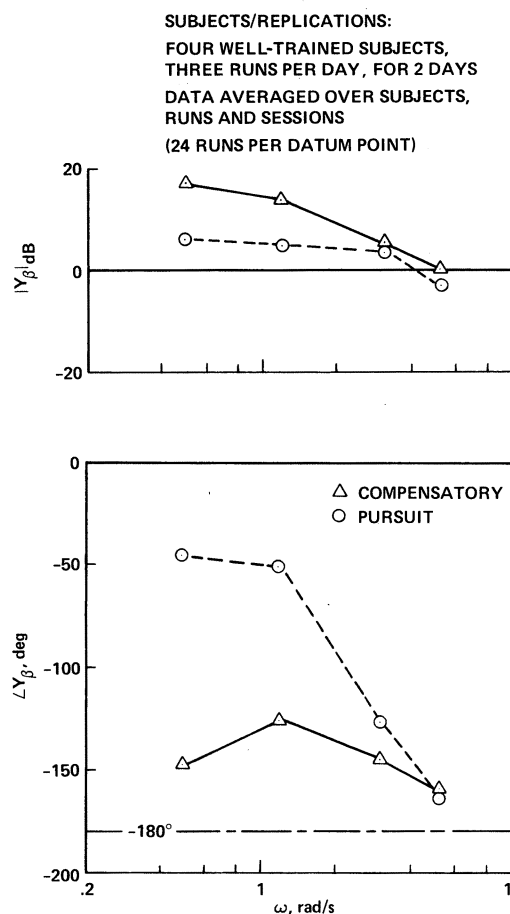


Fig. 5. Comparison of pursuit and compensatory display describing functions from [6].

5, indicate much less low-frequency phase lag for the pursuit than for the compensatory display. In addition, the pursuit display was found to give a lower low-frequency amplitude ratio, a lower crossover frequency, and more phase margin. Although the number of frequencies at which measurements were taken was small, an analysis of variance showed that the differences in data between pursuit and compensatory display cases were statistically signifi-

cant at the two lowest measurement frequencies shown in Fig. 5.

Before proceeding to a model for pilot dynamics with pursuit displays, a brief discussion of pursuit *displays* versus pursuit *behavior* is in order. This is no *a priori* guarantee that the existence of a pursuit display, such as that shown in Fig. 2(b), will induce pursuit behavior on the part of the pilot. When faced with the display of Fig. 2(b), the pilot

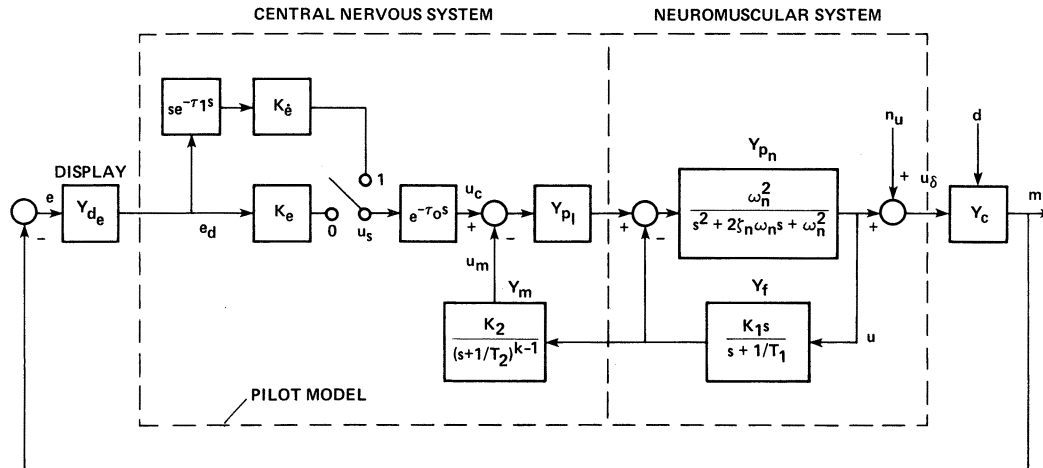


Fig. 6. Structural model of adaptive human pilot for compensatory behavior.

may simply ignore all but the explicit error information and effectively adopt compensatory behavior. Thus detection of pursuit behavior (pilot utilization of more than just error information) with pursuit displays is an important consideration in any experimental effort. A sufficient but not necessary condition for pursuit behavior is that Y_β pursuit differs from Y_β compensatory. Fortunately, the data of [5]–[7] indicate that this sufficiency condition is almost always met. As mentioned previously, these differences are particularly obvious for K/s^2 dynamics. Thus it appears that in all but the exceptional case, the presence of a pursuit display is sufficient to induce pursuit behavior. Likewise, the existence of a compensatory display does not, in theory, preclude the existence of pursuit behavior on the part of the pilot. Indeed, one of the major implications of the SOP theory is that internal stimulus organization may allow the human to utilize input coherency even with a compensatory display. We will have reason to return to this point in the discussion of the motion-cue research.

III. THE COMPENSATORY MODEL

Fig. 6 is a block diagram of a structural model of the human pilot for compensatory behavior. The model was discussed in detail in [9] and shown capable of matching human pilot describing functions and remnant for a wide variety of controlled-element dynamics. Because this compensatory model serves as the basis for the pursuit model to be described shortly, a brief discussion is in order.

The model of Fig. 6 has been divided into “central nervous system” and “neuromuscular system” components, a division intended to emphasize the nature of the hypothesized signal-processing activity. System error $e(t)$ is presented to the pilot via a display with dynamics Y_{de} . The rate of change of the displayed error is assumed to be derived from $e_d(t)$. The process of deriving the error rate is assumed to entail a computational time delay of τ_1 seconds. Constant gains K_e and K_e multiply the signals $e_d(t)$ and $\dot{e}_d(t - \tau_1)$, respectively. The switch allows either of these two signals to be used as driving signals to the remainder of the model. A discussion regarding the utility of error-rate

control is provided in [9]. The action of the switch is parameterized by the variable P_1 , which represents the probability that the switch will be in position 1 (error-rate control) at any instant of time. As discussed in [9], the switching operation can be successfully parameterized by the single quantity P_1 . In a digital simulation of a model generically similar to that of Fig. 6, measured Fourier coefficients were seen to be relatively insensitive to minimum duration of switch closure for a range of values (0.5–5.0s) deemed appropriate for human tracking. A central time delay of τ_0 seconds is included to account for the effects of latencies in the visual process sensing $e_d(t)$, motor nerve conduction times, etc. The resulting signal $u_c(t)$ provides a command to a closed-loop system, which consists of “pulsing logic,” Y_{pl} , a model of the open-loop neuromuscular dynamics of the particular limb driving the manipulator Y_{pn} , and elements Y_f and Y_m , which emulate, at least approximately, the combined effects of the muscle spindles and the dynamics associated with higher level signal processing. A colored noise $n_u(t)$ is injected at the pilot’s output as remnant. A discussion of appropriate pulsing logic was carried out previously by Hess [10] and will not be dealt with here. In this study, $Y_{p1} = 1.0$.

The ability of this compensatory model to provide a match to experimental pilot describing functions is demonstrated by the dashed curves in Fig. 7, which represent the open-loop Y_β obtained via the compensatory model just discussed. The corresponding model parameters are given in the first row of Table I. With the exception of the value of K_e , the parameters shown in the first row of Table I are taken directly from [9], where they were selected to match experimental describing functions from another data source (with K/s^2 controlled-element dynamics, of course). The value of K_e in [9] was simply increased by a factor of 2.5 to obtain the value in Table I. Although a closer fit to the data of Fig. 7 could probably be obtained by varying other parameters, the match will be adequate for the qualitative comparisons to follow.

Nearly all of the pilot’s equalization capabilities (generation of lead, lag, etc.) in the model of Fig. 6 occur through the action of the two loop closures around the open-loop

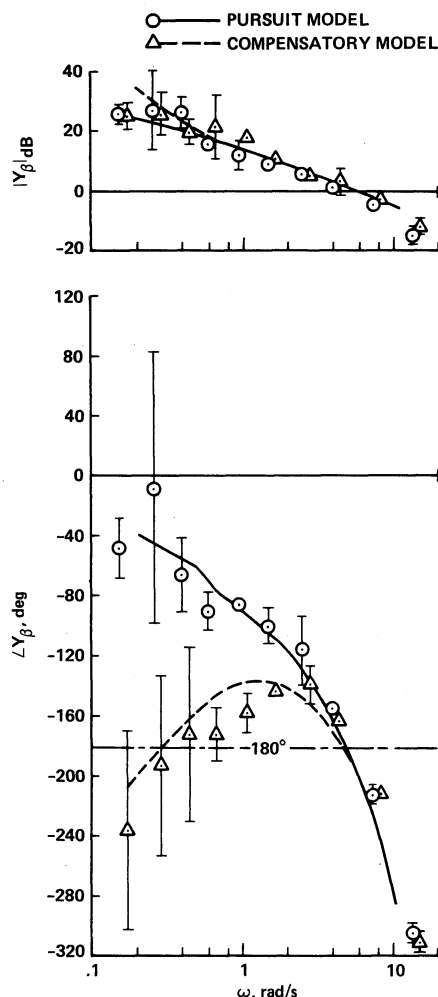


Fig. 7. Comparison of pursuit and compensatory display describing functions from [5] with model describing functions.

neuromuscular system. As pointed out in [9], this equalization is created by an internal model of the controlled-element dynamics implicitly contained in the product $Y_f Y_m$. When the model parameters of Fig. 6 are chosen so that the resulting model describing function is an acceptable representation of actual pilot dynamics, the open-loop describing function is given by

$$K_e \frac{u_\delta}{u_s}(j\omega) Y_c(j\omega) \doteq \frac{(j\omega/a + 1)}{(j\omega/b + 1)} \frac{\omega_c}{j\omega} e^{-j\omega\tau_e} \quad (7)$$

where ω_c is the open-loop crossover frequency, and τ_e is an

effective time delay including the effects of high-frequency closed-loop neuromuscular modes. The right-hand side of (7) is, of course, a form of the "crossover" model of the human pilot for compensatory systems [3]. Equation (7) and Fig. 6 emphasize that no operations, such as differentiation or integration of the displayed error e_d , are necessary in order for the model to develop the required dynamic equalization for compensatory tracking. Thus in terms of the model the variable u_s need not be restricted to system error but can, in theory, be any displayed or derived variable. The utility of using the input rate in this role will be outlined in describing the pursuit model.

Referring to (7) and to Fig. 6, with $k = 2$, ($Y_c = K/s^2$), and $K_1 = 1$ (as in [9]), one can show that

$$a \doteq \frac{1}{(T_2 + 2T_1)} \quad (8)$$

and

$$b \doteq \frac{1}{(T_2 + 2T_1) + K_1(T_1 + K_2 T_2)}. \quad (9)$$

Thus $b < a$ and the lag-lead $(j\omega/a + 1)/(j\omega/b + 1)$ gives rise to the low-frequency characteristics of the compensatory model. Also note that if either T_2 or T_1 (or both) is much larger than unity, then $a \ll 1$ and $b \ll 1$, and in the frequency range of interest for pilot modeling purposes $1 < \omega < 10$ rad/s,

$$K_e \frac{u_\delta}{u_s}(j\omega) Y_c(j\omega) \doteq \frac{\omega_c}{j\omega} e^{-j\omega\tau_e}. \quad (10)$$

This relation is important for the model development that follows.

IV. THE PURSUIT MODEL

The central hypothesis in the development of a pursuit model of the human pilot is that the primary structural elements in the compensatory behavior model also serve as the primary structural elements of the pursuit model. Fig. 8 shows the proposed pilot model for pursuit behavior. It is assumed here that a pursuit *display* is in use also. The primary difference between Figs. 8 and 6 lies in the physical definition of the variable u_s . In the compensatory model, u_s is proportional to error (switch position 0) or to error rate (position 1). In the pursuit model, u_s is postulated to be proportional to a weighted difference of error

TABLE I
PILOT MODEL PARAMETER VALUES USED TO GENERATE
DESCRIBING FUNCTIONS

Controlled- element dynamics	Display	k	K_e	$K_{\dot{e}}$	K_m	$K_{\ddot{e}}$	K_2	P_1	P_2	T_1	T_2	K_1	τ_0	τ_1	ζ_n	ω_n	Y_{P_1}
K/s^2	Comp.	2	65.0	10.5	—	—	10	0.2	—	2.5	2.5	1.0	0.14	0.20	0.707	10	1.0
K/s^2	Pursuit	2	65.0	—	2.5	16.2	10	0.0	0.1	100	100	1.0	0.14	0.20	0.707	10	1.0
$Y_c(s)^*$	Comp.	2	1.5	0.7	—	—	20	0.2	—	0.5	25	1.0	0.14	0.20	0.707	10	1.0
$Y_c(s)^*$	Pursuit	2	1.5	—	0.25	1.1	20	0.0	0.1	0.5	25	1.0	0.14	0.20	0.707	10	1.0

* $Y_c(s) = 17 \frac{(-s/25 + 1)}{s(s/1.6 + 1)(s/5 + 1)(s^2/121 + 6.6s + 1)}$

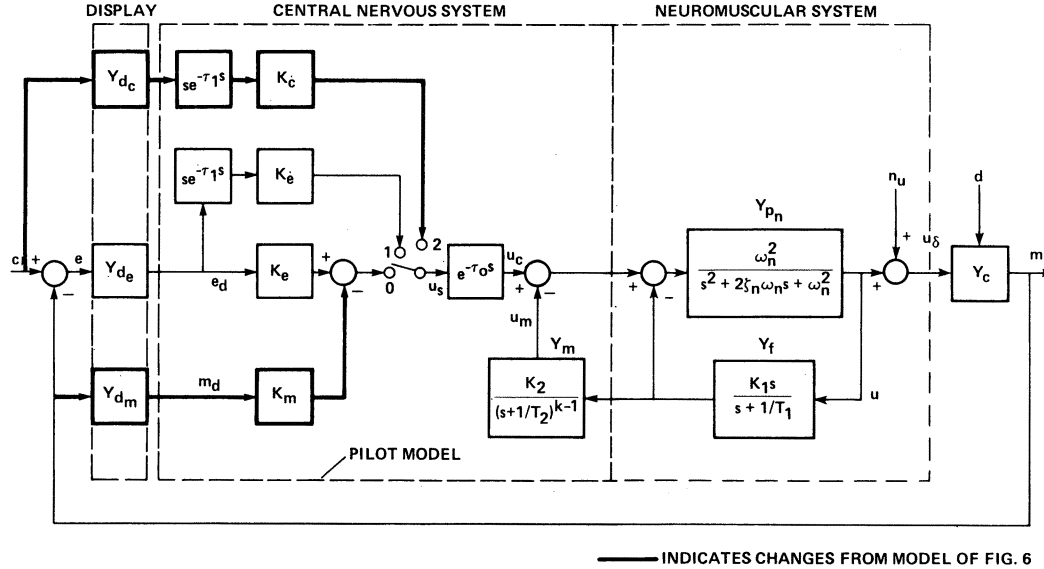


Fig. 8. Structural model of adaptive human pilot for compensatory-pursuit behavior.

and output (position 0), to error rate alone (position 1), or to input rate alone (position 2). As was the case in the compensatory model, the input rate is assumed to be a derived quantity with a time delay τ_1 associated with the rate calculation. In the model of Fig. 8, the operation of the switch will be parameterized by P_1 and P_2 , the respective probabilities of switch being in position 1 or 2 at any instant. The probability of its being in position 0 is, of course, simply $1 - P_1 - P_2$. Note that by allowing $Y_{dm} = Y_{dc} = P_2 = 0$, the pursuit model becomes identical to the compensatory model and thus encompasses it.

Now the feed-forward of the input rate through the dynamics $u_\delta(j\omega)/u_s(j\omega)$ can effectively invert the controlled-element dynamics at low frequencies. Referring to (10), which assumes that low-frequency phase droop has been minimized,

$$m(j\omega) = K_c(j\omega)c(j\omega)\frac{1}{K_e}\frac{\omega_c}{j\omega}e^{-j\omega(\tau_e+\tau_1)}. \quad (11)$$

With $K_c = K_e/\omega_c$, we have, for frequencies small when compared to $1/(\tau_e + \tau_1)$,

$$m(j\omega) \doteq c(j\omega). \quad (12)$$

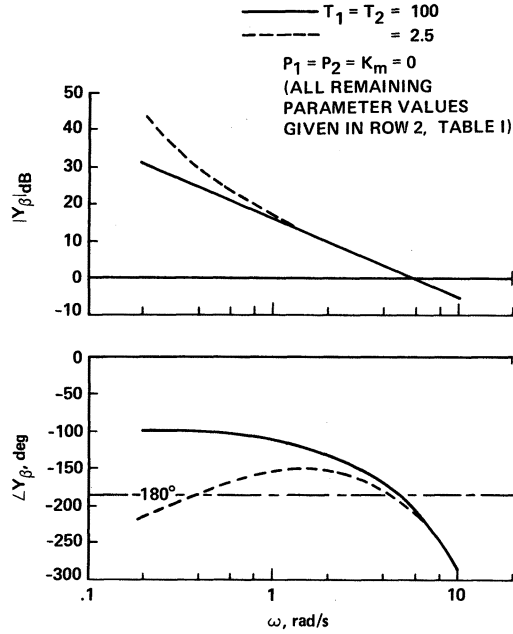
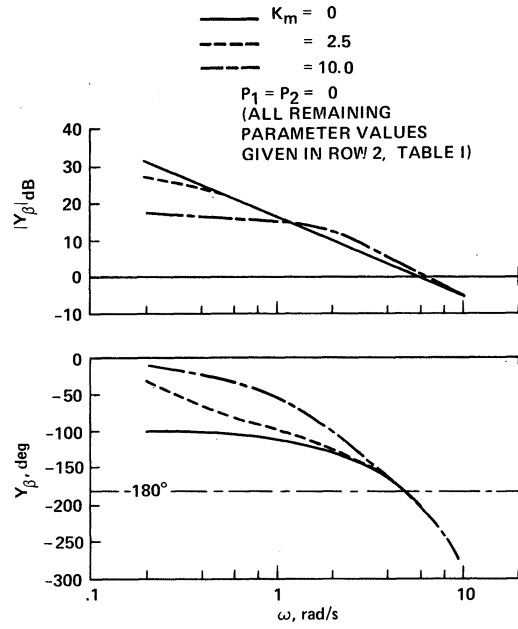
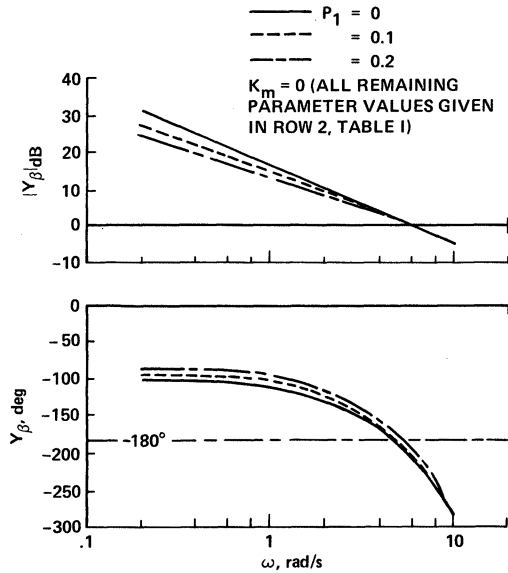
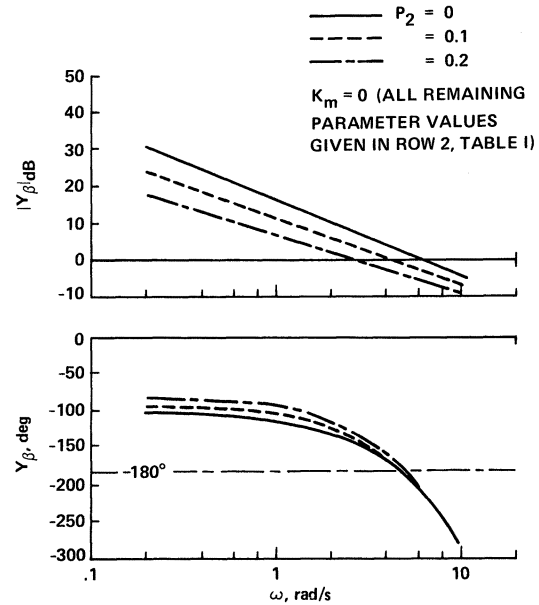
This implies low-frequency inversion of the controlled-element dynamics between $c(t)$ and $u_\delta(t)$ in Fig. 8 with the switch in position 2. We will now give some quantitative evidence of the ability of the model of Fig. 8 to yield describing functions that produce effective open-loop dynamics comparable to the Y_β measurements of [5]. In addition, we will provide a rationale for the use of output feedback in the model.

Fig. 7 shows a comparison of the pursuit display describing functions from [5] with the describing functions obtained from the pursuit model of Fig. 8, using the parameter values shown in Table I. The model describing functions with the two-position switch in operation were obtained by using an approximation procedure discussed in some detail in [9]. Note the model's ability to capture

the large low-frequency phase differences. Note also that the low-frequency amplitude ratio of the pursuit display task is less than that of the compensatory. The decrease in crossover frequency and increase in phase margin noted in the pursuit data of [6] is not evident in the data of [5], which were used to select model parameters. Consequently, the model describing functions do not exhibit these characteristics.

Table I indicates that five parameter values were changed in going from the compensatory to the pursuit case in achieving the matches of Fig. 7. First, K_m and K_c take on nonzero values, the first of which is an order of magnitude smaller than K_e . The probability of input-rate feed-forward being utilized, P_2 , has been set to 0.1, and P_1 , the probability of error-rate tracking occurring, is negligible. Finally, both T_1 and T_2 have been increased from 2.5 to 100 to effectively minimize phase droop when the switch is in position 2.

Figs. 9–12 demonstrate how the variation in T_1 ($T_2 = T_1$), K_m , P_1 , and P_2 affect Y_β . As Fig. 9 shows, increasing T_1 from 2.5 to 100 (with $K_m = P_1 = P_2 = 0$ and with the remaining parameter values as in row 2 of Table I) effectively removes the low-frequency phase droop and causes a concomitant reduction in low-frequency amplitude ratio. Fig. 10 shows the effect of K_m variation. As K_m is increased, low-frequency phase lags are sharply reduced, and reductions in low-frequency amplitude ratio occur. It should be noted that in terms of their effect on Y_β , the parameters T_1 and K_m are not interchangeable; that is, one cannot eliminate phase droop with K_m alone and create phase lead with T_1 alone. The comparatively small effect of P_1 variation (error-rate tracking) is shown in Fig. 11. Note from this figure that the use of intermittent error-rate information is not equivalent to utilizing a continuous combination of error and error rate (simple lead generation). The latter would be accompanied by a definitive 20-dB per decade change in the slope of the Y_β curves, not evident in Fig. 11. Fig. 12 shows how variations in P_2 (input-rate feed-forward)

Fig. 9. Effects of T_1, T_2 variation in pursuit model describing functions.Fig. 10. Effects of K_m variation in pursuit model describing functions.Fig. 11. Effects of P_1 variation in pursuit model describing functions.Fig. 12. Effects of P_2 variation in pursuit model describing functions.

affect Y_β . Here, significant and nearly frequent-invariant reductions in open-loop gain accompany increases in P_2 .

A plausible explanation for the pilot's use of output feedback can now be obtained by considering approximations to the Y_β functions of Fig. 10 for $K_m = 0$ and $K_m = 10$. For $K_m = 0$ and ignoring the time delay τ_0 ,

$$Y_\beta \doteq \frac{6}{s}.$$

Similarly, for $K_m = 10$

$$Y_\beta \doteq \frac{4}{s/2 + 1}.$$

Now the approximate *closed-loop* transfer functions for

each of these Y_β 's are

$$\left. \frac{m}{c} \right|_{K_m=0} \doteq \frac{6}{s+6}$$

and

$$\left. \frac{m}{c} \right|_{K_m=10} \doteq \frac{8}{s+10}.$$

Output feedback is thus seen to increase the system bandwidth from approximately 6 to 10 rad/s. This bandwidth increment is important because, as Fig. 12 indicates, pursuit behavior would *lower* the open-loop crossover frequency considerably without output feedback (Fig. 10 was obtained with $P_2 = 0$). This would, in turn, lower the closed-loop bandwidth. However, the output feedback also lowers

the static gain of the closed-loop system from the desirable unity to a value of 0.8. This is attributable to the low-frequency Y_β amplitude ratio reduction evident in Fig. 10. This gain reduction is clearly evident in the experimental closed-loop describing function measurements of [5] and [6].

The procedure for selecting the model parameters to yield the matches of Fig. 7 was *ad hoc* in nature and no formal numerical criterion was employed to determine the quality of the fit; that is, it was determined visually. The procedure went roughly as follows. First, the parameter values from the K/s^2 fit in [9] were selected, and K_e was increased to obtain the describing function indicated by the dashed curves in Fig. 7. This completed the compensatory match. For the pursuit case, the relation $K_c = K_e/\omega_c$ allowed immediate determination of K_c . The parameter T_1 ($T_2 = T_1$) was set to a sufficiently large value to minimize low-frequency phase droop, the value $T_1 = 100$ serving nicely. Selecting a value for K_m was accomplished by obtaining an acceptable match to the pursuit low-frequency phase data in Fig. 7. Since Figs. 9–11 indicate that the effect of P_1 on the Y_β functions is comparatively small, we allow $P_1 = 0$. This also obviates selection of K_e . It should be noted that remnant data would probably allow determination of a P_1 value as was the case for the compensatory mode of [9]. The value of $P_2 = 0.1$ represents more of an *a priori* assumption rather than a parameter estimate. In terms of the model of Fig. 8, pursuit behavior implies a finite probability of open-loop activity involving the perceived input. Selecting $P_2 = 0.1$ was felt to be a reasonable estimate for such open-loop activity.

Obviously, this *ad hoc* parameter selection procedure is not meant to imply unique parameter *identification*. We are simply demonstrating that the model structure of Fig. 8 can yield describing functions that provide acceptable matches to available frequency domain data.

The potential of the model just discussed lies in its ability to provide a more satisfactory structural representation of pursuit behavior than that offered by models such as the one shown in Fig. 3 (whose structure was formulated to ease the burden of identification). For example, with K/s^2 dynamics, successful inversion of Y_c in the model of Fig. 3 implies that the pilot continuously provides double lead equalization ($Y_{p_c} = s^2/K$), a factor long associated with totally unacceptable pilot workload. Other forms of Y_c , such as that associated with aircraft phugoid and short-period dynamics, would imply even more complex equalization in Y_{p_c} , but [5] and [6] clearly indicate pilot preference for the pursuit rather than the compensatory display for these dynamics. Hence we are presented with something of a contradiction in trying to interpret the empirical phenomena of pilot preference for pursuit displays in light of the theoretical framework provided by the model of Fig. 3; however, no contraction exists with the model of Fig. 8. No matter what the form of Y_c , effective inversion can be accomplished by feeding-forward input-rate. In addition, the model does not demand continuous

use of the input rate (first-order lead equalization) since P_2 only equals 0.2 in Table I.

V. SOME RESULTS FROM MOTION-CUE RESEARCH

Some recent research involving a single-axis piloted tracking task that was performed on a motion simulator constrained to rotate about the longitudinal or roll axis is summarized in [11]. In an air-to-air tracking scenario, the task consisted of following the target's roll angle while suppressing gust disturbances. Fig. 13(a) and (b) show, respectively, a block diagram of the tracking task and the pilot's compensatory visual display consisting of a rotating "target wing" whose center was superimposed upon a stationary horizontal dashed line. Fig. 14 illustrates the frequency characteristics of the vehicle dynamics (ϕ/δ transfer function). Also shown is the required approximation to these dynamics in the form Ks^{-k} , valid in the frequency range near open-loop crossover ($\omega_c \doteq 1.3$ rad/s from [11]). The determination of k ($k = 2$) is necessary for the implementation of the models of Figs. 6 and 8.

The experiments were performed with 1) no motion, 2) with full motion and the roll axis horizontal (pilot nominally erect), 3) with full motion and the roll axis vertical (pilot nominally supine), 4) with washed-out motion, and 5) with attenuated motion. The latter two conditions were studied with the roll-axis horizontal. The first and third of these experiments, and to some extent the fourth, were designed to suppress the so-called "tilt cue" which the pilot receives when tracking with full motion and the roll-axis horizontal. This cue arises from vestibular sensors in the inner ear. A rather sophisticated parameter identification algorithm was implemented in [11] to allow a 12-parameter pilot model to match the measured describing functions. The quality of the matches was such that for our purposes we can consider the model describing functions (continuous over frequency) as representing actual data.

Fig. 15 and 16 summarize the describing functions for the experiments just described. Two distinct describing functions were measured for each experimental condition, one corresponding to the Y_β discussed previously (ϕ_e/ϕ in Fig. 13), and a second corresponding to δ_1/δ in Fig. 13. Only the first of these will be discussed here since these tie in with the measurements made by Wasicko *et al.* [5].

The first thing that draws our attention to these data is the qualitative similarity in the changes in low-frequency phase and amplitude ratio between the various motion conditions of Figs. 15 and 16, and the compensatory and pursuit display conditions of Fig. 4. With the notable exception of the absence of low-frequency phase droop, the static (ST), full-motion-supine (F90), and full-motion-erect-with-washout (W1, W1A, W2) cases can be likened to the compensatory data of Fig. 4; the full-motion-erect (F0) and attenuated-motion (ATT) cases can be likened to the pursuit data.

If we extend our concept of "display" to include vestibular cues, the experimental conditions of [11] are quite

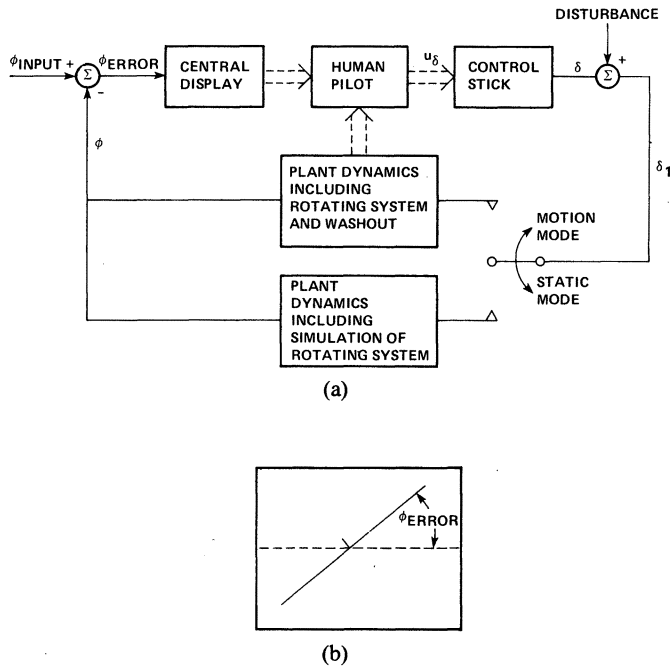


Fig. 13. Experimental tracking task of [11]. (a) Block diagram. (b) Display.

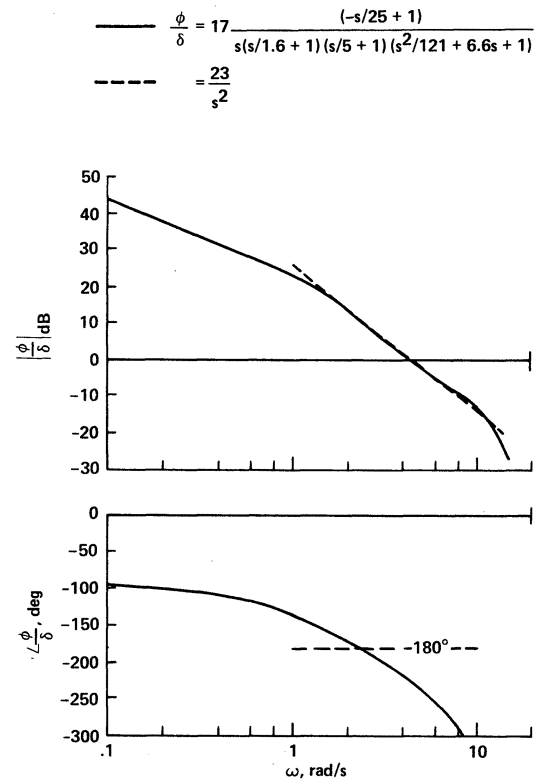


Fig. 14. Vehicle dynamics for roll tracking task of [11].

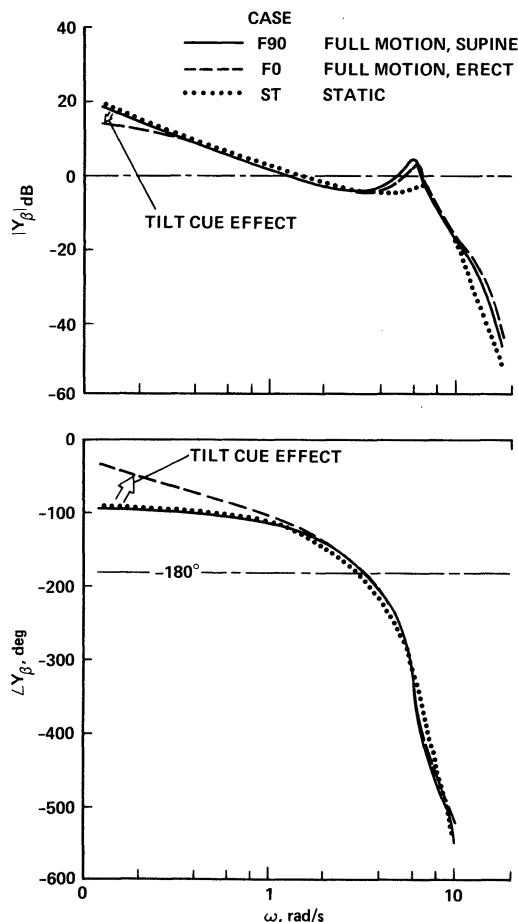


Fig. 15. Comparison of experimental describing functions from [11].

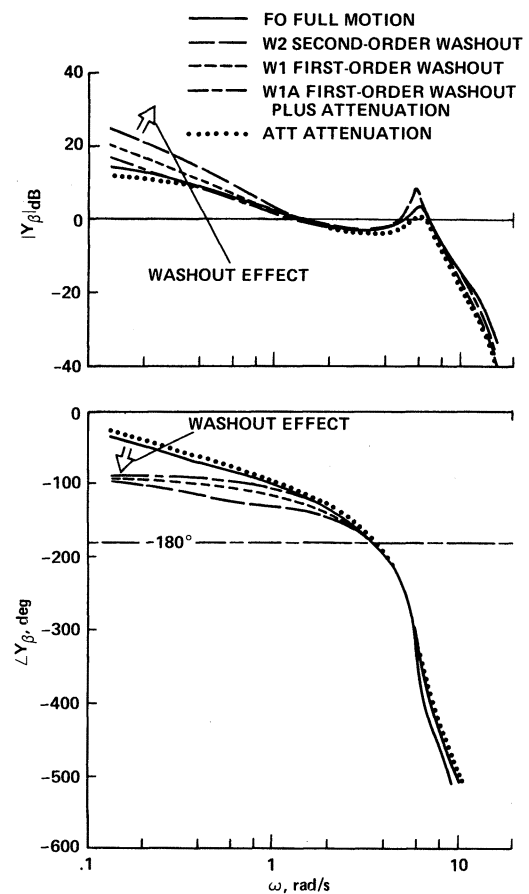


Fig. 16. Comparison of experimental describing functions from [11].

TABLE II
EFFECTIVE DISPLAY CONDITIONS FOR EXPERIMENTS OF [11]

Experimental Condition from [11]	"Displayed" Variables	Effective "Display" Condition
Static (ST)	ϕ_e	Compensatory
Full motion erect (F0)	$\phi, \phi_e, \dot{\phi} \dots *$	Pursuit
Full motion supine (F90)	$\phi_e, \dot{\phi} \dots$	Compensatory
Motion washout (W1, W1A, W2)	$\phi_e, \dot{\phi} \dots$	Compensatory
Motion attenuation (ATT)	$\phi, \phi_e, \dot{\phi} \dots$	Pursuit

*. . . denotes higher order derivatives sensed via vestibular system.

similar to the compensatory and pursuit tracking displays discussed previously. This is emphasized in Table II, in which the various experimental conditions are listed with their corresponding effective display conditions. In the static case (ST), of course, the only display is visual and compensatory in nature; that is, ϕ_e alone is displayed. In the full-motion-erect case, the vestibular "tilt cue" is available as an additional display element, effectively giving the pilot information about the controlled-element output ϕ in addition to the displayed error ϕ_e , thus yielding a pursuit display. In addition, the F0 case may allow higher derivatives of ϕ to be sensed [12], but the effect of this feedback will be beyond the frequency range of interest here ($\omega < 4$ rad/s) [11]. When the cab is rotated 90° (F90), the tilt cue is no longer available to the pilot, leading to a compensatory display. As the name implies, the various motion washouts (W1, W1A, and W2) were designed to wash out the low-frequency controlled-element output ϕ . Because the washouts eliminated motion in the frequency range in which the target input contained most of its power, we can say that qualitatively the washouts led to an effective compensatory display again. Finally, in the motion-attenuation case, a pursuit display is created since the attenuation merely serves to lower the gain of the cab's motion system.

Fig. 17 illustrates the model-generated describing functions corresponding to the controlled-element dynamics of Fig. 14 and the models of Fig. 6 and 8. The corresponding model parameters are listed in the last two rows of Table I. Model parameters were selected using the technique discussed in [9]. Strictly speaking, only the static case (ST of Fig. 15) should be subject to comparison because the models of Figs. 6 and 8 are not specifically formulated for motion cues involving higher derivatives of the vehicle output. If we restrict our attention to the lower frequencies ($\omega < 4$ rad/s), however, a qualitative, if not quantitative, comparison of modeling results when the experimental motion data are reasonable. As Fig. 17 indicates, the model can capture the salient differences in the experimental data in terms of the compensatory-pursuit dichotomy suggested by Table II. One point should be noted regarding the T_1, T_2 values in the last two rows of Table II. Acceptable matches to the experimental Y_β measurements could not be achieved allowing $T_1 = T_2$, as was the case with the K/s^2 dynamics.

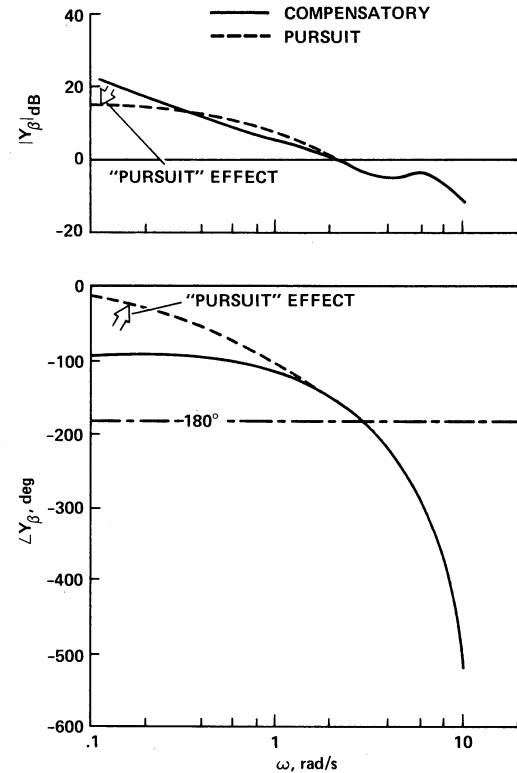


Fig. 17. Comparison of pursuit and compensatory model describing functions.

In eliminating model phase droop, T_2 had to be increased alone.

One of the more interesting facets of the data of Figs. 15 and 16 is the complete absence of phase droop, even with a compensatory display; for example, ST. This somewhat anomalous result was mentioned in [11], but no explanation was offered. Based on the model discussed here, two speculative explanations can be given.

1) A transfer of training from the pursuit motion conditions is occurring in which the pilots are minimizing phase droop for the pursuit cases and maintaining the "set" for the compensatory cases.

2) Higher levels of skill development are being attained with the compensatory display, and the subjects are tailoring their dynamic characteristics to take advantage of any input coherency that they detect during their extensive training. It is pertinent to note that the input consisted of a sum of eight sinusoids and was unchanged throughout the training and experiments. The absence of explicit and continuous output information with the compensatory display would, of course, preclude any further reductions in low-frequency phase lags over and above that associated with elimination of droop.

This limited discussion of motion-cue research has emphasized the concept that in tracking tasks the human pilot can be viewed as a data-organizing device. This organization tends to be independent of the physical nature of the display and proceeds along lines suggested by the model of Fig. 8. That is, sensory stimuli tend to be utilized in a manner that allows the pilot to progress from compensatory to pursuit behavior. In the next section we

discuss stimuli that allow even further progression in skill development.

VI. TRACKING WITH PREVIEW AND PRECOGNITIVE BEHAVIOR

Fig. 18 is a schematic representation of a display allowing tracking with preview (and postview). The curve represents the input, which moves from right to left, past the tracking symbol, and disappears off the screen to the left. The subject's task is to keep the small circular tracking symbol (constrained to move in the vertical direction only) on the input track. If the amount of preview and postview is reduced to 0s, a pure pursuit display results. Thus pursuit tracking is a limiting case of tracking with preview.

Preview tracking has received even less attention in the literature than pursuit tracking despite the fact that a great deal of manual control—from day-to-day experiences such as automobile driving to terrain following tasks in advanced aircraft—involves preview. However, the problem of tracking with preview has been studied, and models for the task have been proposed, e.g., [13]–[19]. In terms of the model that has been discussed here (Fig. 8), preview would result in improved tracking performance, primarily by allowing reduction of the open-loop time delay $\tau_1 + \tau_e$, which occurs in feeding-forward input-rate. Theoretically, this delay can be reduced or completely eliminated through preview by allowing the subject to estimate $\dot{c}(t)$ at $t = t_0 + \tau_1 + \tau_e$. The nature of this rate estimation could be spatial, a combination of spatial and temporal, or purely temporal. In the former case, the segment of input available for observation would allow the operator to utilize the shape of the waveform to generate $\dot{c}(t)$. In the latter case, only the instantaneous behavior of $\dot{c}(t)$ would be utilized. The precise nature of $\dot{c}(t)$ estimation will not be hypothesized here, however, as it is not of particular importance to the discussion which follows. A rough estimate of $\tau_1 + \tau_e$ can be obtained from [9], and for the purposes of a comparison with the data of [14], we will concentrate on values of τ_e appropriate for K/s dynamics:

$$\tau_0 \doteq 0.15 \text{ s (independent of dynamics)}$$

$$\tau_e = \tau_0 + \Delta\tau \doteq 0.2 \text{ s } (\Delta\tau \text{ dependent on dynamics})$$

and

$$\tau_1 \doteq 0.2 \text{ s (independent of dynamics).}$$

Here we have made the conservative estimate that derivation of estimation of $\dot{c}(t)$ with a preview display will still involve a computational time delay of 0.2 s; thus $\tau_1 + \tau_e \doteq 0.4$ s. The 0.2-s value is an estimate of the sampling delay inherent in a “differential-displacement” model of rate derivation [20]. It is quite probable that the nature of $\dot{c}(t)$ estimation will effect the magnitude of τ_1 and the 0.2-s value represents an upper limit. It was shown in [14] and [15] that significant performance improvements do accrue with preview, and that almost all improvement is obtained between 0.3 and 0.7 s. As a specific example, Fig. 19 (from [14]) shows the performance improvements for a well-trained subject versus preview time with K/s dynamics and

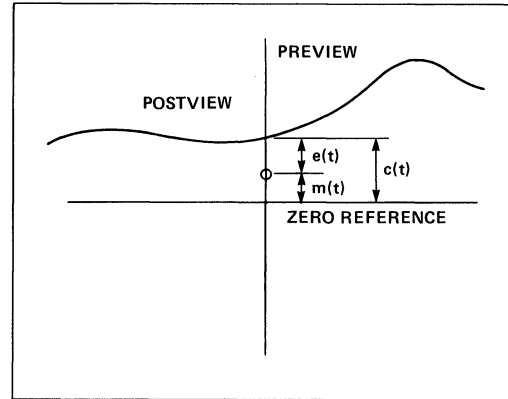


Fig. 18. Schematic view of preview display.

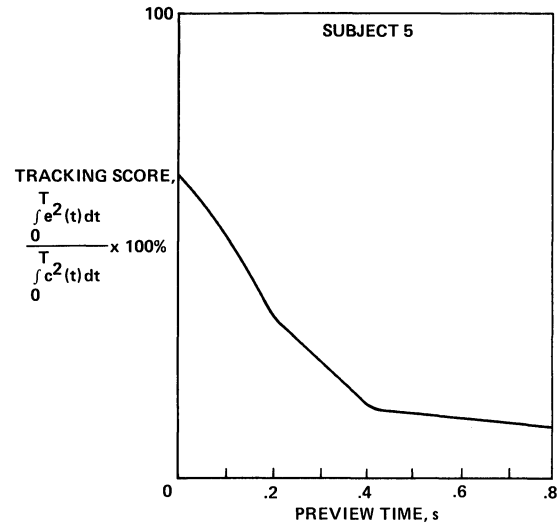


Fig. 19. Typical tracking score improvement versus preview time for trained subject [14].

the display of Fig. 18. As the figure shows, preview times greater than 0.4 s do not yield significant performance improvements.

In terms of the model of Fig. 8, a preview display allows the effective inversion of the plant dynamics to be more broad-band than the inversion that would accompany a pursuit display. If one generalizes the concept of a preview display to include an input waveform or stimulus *internally* generated by the pilot in the higher levels of the central nervous system, then the structure of Fig. 20 can serve as a paradigm for manual control behavior not considered as tracking activity *per se*; that is, the “precognitive” mode viewed by Krendel and McRuer [2] as the highest form of skill development. Fig. 20, a slight modification of Fig. 8, now includes the possibility of the pilot internally generating a $c(t + \tau_1 + \tau_e)$ signal. Note that Fig. 20 encompasses all the models that describe lower levels of skill development or display utilization.

VII. CONCLUDING REMARKS

A model of the human pilot has been offered for pursuit tracking tasks; the model encompasses the model for compensatory tasks introduced in [8] and refined in [9]. The central hypothesis in the development of this model is that

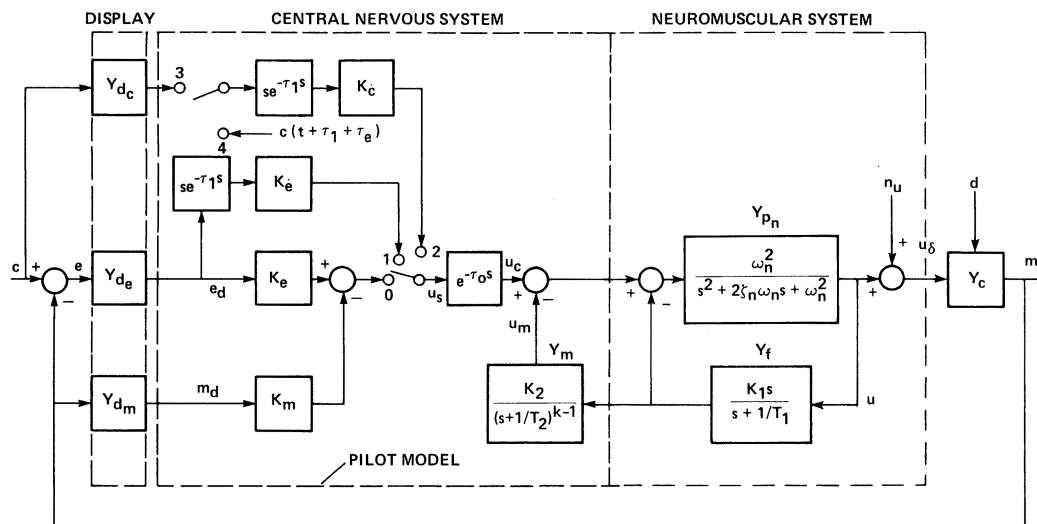


Fig. 20. Structural model of adaptive human pilot for compensatory-pursuit precognitive behavior.

the structural elements in the compensatory model that are responsible for the pilot's equalization capabilities remain intact in the pursuit model. In this latter case, effective low-frequency inversion of the controlled element dynamics occurs by way of feeding-forward derived input-rate through the equalization dynamics u_s/u_s with low-frequency phase droop minimized. The sharp reduction in low-frequency phase lags beyond the reduction associated with the disappearance of phase droop was seen to accompany relatively low-gain feedback of vehicle output. After demonstrating that the model can capture the salient frequency domain characteristics of pursuit behavior, the results of some recent motion-cue research were discussed and interpreted in terms of the compensatory-pursuit display dichotomy. Tracking with input preview was discussed in qualitative fashion. In terms of the model, preview was seen not to demand any fundamental changes in structure or equalization but rather to allow the pilot to eliminate the time delays that occur in the open-loop tracking. This, in turn, allows effective inversion of the controlled-element dynamics over a broader frequency range than that possible with a pursuit display alone. Precognitive behavior was discussed, and a single model encompassing all the levels of skill development outlined in [2] was proposed.

The utility of the model proposed here does not lie in its predictive capability in the sense of generating performance estimates, nor in its ability to offer a structure involving the minimum number of parameters necessary to simulate measured pilot frequency domain characteristics in a particular task. Rather, its value lies in its ability to serve as a tool for unifying the entire base of single-axis tracking data and to provide a structure for understanding aspects of motor skill development.

REFERENCES

- [1] E. C. Poulton, *Tracking Skill and Manual Control*. New York: Academic, 1974, ch. 9.
- [2] E. S. Krendel and D. T. McRuer, "A servomechanisms approach to skill development," *J. Franklin Inst.*, vol. 269, pp. 24-42, Jan. 1960.
- [3] D. T. McRuer, D. Graham, E. Krendel, and W. Riesener, Jr., "Human pilot dynamics in compensatory systems," Air Force Flight Dynamics Lab., Rep. AFFDL-TR-65-15, 1965.
- [4] J. I. Elkind, "Characteristics of simple manual control systems," MIT Lincoln Lab., Tech. Rep. 111, Apr. 1956.
- [5] R. J. Wasicko, D. T. McRuer, and R. E. Magdaleno, "Human pilot dynamic response in single-loop systems with compensatory and pursuit displays," Air Force Flight Dynamics Lab., Rep. AFFDL-TR-66-137, 1966.
- [6] R. W. Allen and H. R. Jex, "An experimental investigation of compensatory and pursuit tracking displays with rate and acceleration control dynamics and a disturbance input," NASA CR-1082, 1968.
- [7] L. D. Reid, "An investigation into pursuit tracking in the presence of a disturbance signal," in *Proc. 5th Annu. Conf. Manual Control*, Mar. 1969, pp. 129-169.
- [8] R. A. Hess, "A dual-loop model of the human controller," *J. Guidance Contr.*, vol. 1, pp. 254-260, July-Aug. 1978.
- [9] —, "A structural model of the adaptive human pilot," *J. Guidance Contr.*, vol. 3, pp. 416-423, Sept.-Oct. 1980.
- [10] R. A. Hess, "A rationale for human operator pulsive control behavior," *J. Guidance Contr.*, vol. 2, pp. 221-227, May-June 1979.
- [11] H. R. Jex, R. E. Magdaleno, and A. M. Junker, "Roll tracking effects of G-vector tilt and various types of motion washout," in *Proc. 14th Annu. Conf. Manual Control*, Apr. 1978, pp. 463-502.
- [12] W. H. Levison and A. M. Junker, "A model for the pilot's use of motion cues in roll-axis tracking tasks," Aerosp. Med. Res. Lab., Rep. AMRL-TR-77-4, June 1977.
- [13] T. B. Sheridan, "Three models of preview control," *IEEE Trans. Hum. Factors Electron.*, vol. HFE-7, pp. 91-102, June 1966.
- [14] L. D. Reid and N. H. Drewell, "A pilot model for tracking with preview," in *Proc. 8th Annu. Conf. Manual Control*, May 1972, pp. 191-204.
- [15] M. Tomizuka and D. E. Whitney, "The human operator in manual preview tracking (An experiment and its modeling via optimal control)," *ASME J. Dynamic Syst., Meas., Contr.*, pp. 407-413, Dec. 1976.
- [16] E. Donges, "A two-level model of driver steering behavior," *Hum. Factors*, vol. 20, pp. 691-707, 1978.
- [17] T. Govindaraj and W. B. Rouse, "Human controller modeling in environments that include non-control tasks," in *Proc. 18th Conf. Decision and Control*, Dec. 1979, pp. 989-994.
- [18] J. G. Kreifeldt, "An analysis of the human as a predictor model," in *Proc. 18th Conf. Decision and Control*, Dec. 1979, pp. 1074-1077.
- [19] D. R. Arnott and T. Govindaraj, "Does Man always close the loop in trying to pilot a large ship?" in *Proc. 16th Annu. Conf. Manual Control*, May 1980, pp. 533-539.
- [20] D. T. McRuer et al., "New approaches to human pilot/vehicle dynamic analysis," Air Force Flight Dynamics Lab., Rep. AFFDL-TR-67-150, 1968.